Experimental study of the structure of the lean two-dimensional hydrogen-methane-air Bunsen flame tip with implications to turbulent flames

Y.L. Shoshin*[1], A.V. Sepman[2], L.P.H. de Goey[1], A.V. Mokhov[3], and H.B. Levinsky[3].

[1]Eindhoven University of Technology, The Netherlands
[2]SP Energy Technology Centre, Piteå, Sweden
[3]University of Groningen, The Netherlands

Abstract

Flame cusps, or folds, which form on concave fragments of turbulent flames are locations of strong negative flame stretch. In mixtures with non-unity Lewis number, in particular, in hydrogen-containing mixtures, local flame stretching induces preferential diffusion, which may affect such practically important characteristics as local burning velocity, flame temperature and reaction rates. In present work, the detailed structure of flame cusps represented by the tip of 2-dimensional laminar Bunsen flames of lean (H2+CH4)-air mixtures has been studied experimentally using spontaneous Raman scattering.

Introduction

When curved flames propagate into a fresh mixture of reactants, cusps may form on concave fragments of the flame front as a result of the local flame front propagation relative to the gas. In particular, cusps are commonly formed in turbulent flames, because the flame front is deformed by the turbulent flow. Cusp formation is intensified in mixtures with Lewis numbers less than unity due to the flame cellular instability.

Flame cusps are locations of strong negative flame stretch induced by the large local curvature of the flame front. In mixtures with non-unity Lewis number, preferential diffusion is induced by these stretch phenomena, which may significantly affect the local burning rates and flame temperature. As a consequence, the overall burning rate, the completeness of combustion and the levels of pollutant emissions may also be affected [1,2]. This is in particular relevant to the practically important case of turbulent flames of lean hydrogen-containing fuel gas mixtures, which have an "effective" Lewis number less than unity.

The tip of a 2-D Bunsen flame is essentially a flame front cusp, which is produced in a very controllable and convenient way for diagnostics. A number experimental and theoretical investigations have been reported on the effects of the Lewis number on the structure of the Bunsen flame tip for mixtures containing a single fuel, or single Lewis number mixtures, see e.g. [3,4]. The structure of Bunsen flame tips in (H2+CH4)-air mixtures, however, to our knowledge, has not been investigated. In the present work, the detailed structure of flame cusps represented by the tip of a 2-dimensional laminar Bunsen flame propagating in lean (H2+CH4)-air mixtures has been studied experimentally. Flame temperature and molar fractions of major species were measured using spontaneous Raman scattering. Besides, flame images were recorded by a video camera equipped with a CH* optical filter. Local maximal image intensities registered with the CH* filter have been determined at the flame tip and at the flame shoulder and their ratio was considered as a qualitative indicator of the strength of flame stretch effects at the flame tip. Lean mixtures of air with methane and with fuel blends of methane and hydrogen have been tested.

Experimental setup

Flames were stabilized at very lean conditions, to provide their large diffusion thickness and to be able to resolve the detailed structure of the flame apex. Figure 2 shows a schematic of the burner used in the experiments. The burner has seven slots of 4 x 30 mm cross section, separated by a 4 mm distance. The multi-slot burner configuration has been chosen instead of a single-slot one because it allows stabilizing much leaner flames due to mutual support of neighbor flames. The three central flames stabilized on the burner were nearly identical. The central flame was used for measurements. The mixture flow is evenly distributed among the slots and along each slot using a plate with double rows of equally spaced 0.5 mm diameter holes positioned along each slot entrance. Flow straighteners are installed inside each slot before the burner exit, which prevents flow turbilization after passing of the mixture through small holes, and forms near-uniform mixture velocity profiles at the burner exit.

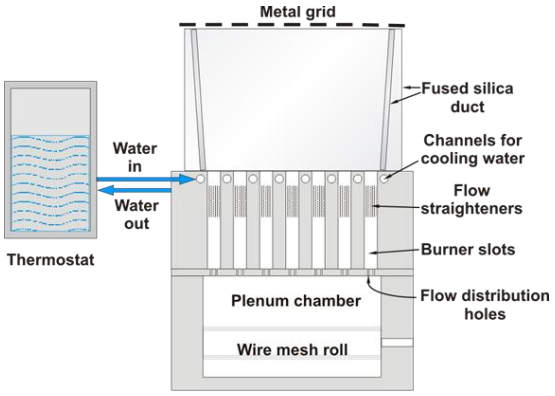

Figure 1. Schematic of the multi-slot laminar burner used in the experiments.

* Corresponding author: y.s.shoshin@tue.nl

A wire mesh roll surrounding the mixture inflow port is installed in the plenum chamber to quench turbulence inside the chamber and to remove pressure pulsations, which otherwise would disturb the flames.

Table 1. Mixtures used in the experiment

S_b, cm·s^{-1}	φ, CH_4/air	φ, $(0.8CH_4+0.2H_2)$/air	φ, $(0.6CH_4+0.4H_2)$/air	φ, $(0.4CH_4+0.6H_2)$/air
7			0.495	0.45
10	0.588	0.569	0.528	0.492
15	0.647	0.619	0.58	
20	0.711	0.674	0.631	

A duct made of fused silica plates is installed above the burner outflow plane to protect flames from occasional drafts and to further extend flame stabilization limits. To keep the burner surface at a constant temperature, thermostated water is pumped through the cooling channels drilled close to the burner top surface.

Tested mixtures were prepared in-line from high purity cylinder gases (hydrogen, methane, and dry synthetic air), using mass-flow controllers installed in each gas line (not shown in Fig. 1). The three flows are then combined in one.

Flame images were taken with a Pike AVT PIKE F-032B BW video camera equipped with an interference filter with the transmission range 432±10 nm (CO* bands). Gray-scale images of 14 bit scale ware taken. The same camera aperture and exposure was used for all chemiluminescence measurements.

The flame temperature and major species (CO, CO2, N2, H2, H2O, CH4 and O2) were measured using spontaneous Raman scattering. The optical scheme and the procedure for deriving flame temperature and major species concentrations by fitting measured Raman spectra is described in detail in [5]. Here, we discuss it only briefly. The exciting laser beam from a Nd:YLF laser (Spectra Physics Empower, 5 kHz repetition rate, 400 ns pulse duration and an average power of 30 W at a wavelength of 527 nm) was focused in at the flame by a lens with focal length of 500 mm. The scattered radiation was collected at right angles by a f/2.8 lens with focal length of 300 mm. The scattered radiation was dispersed by an f/4 spectrometer (Acton Research Spectra Pro 2300i), which was oriented such that its entrance slit was parallel to the exciting laser beam. Before entering the spectrometer, the radiation was directed through the filter and a vertical polarizer. The 2400 mm-1 and 300 mm-1 gratings were used for the temperature and concentration measurements, respectively. The measured N2 spectra were used for fitting the temperature. In the present study, 20 pixels were binned along the axis of the laser beam, integrating the signal over distances of roughly 0.5 mm, yielding the radial spatial resolution of the experiment.

Line-wise measurements have been performed at selected horizontal levels above the burner. Temperature profiles were determined with a constant vertical step of 1 mm. In case of species measurement, the vertical step between the selected levels varied from 2 mm at the flame tip to 3 mm at the flame shoulders. 2-D distributions of measured values were then plotted using linear interpolation between the selected horizontal levels.

Results and discussion

Mixture compositions used in the experiment are described in Table 1. Equivalence ratios were selected, which correspond to theoretical burning velocities of the adiabatic planar flames of S_b = 7, 10, 15, and 20 cm·s^{-1}, determined using the Chem1D code [6] and the GRI-3.0 reaction mechanism [7].

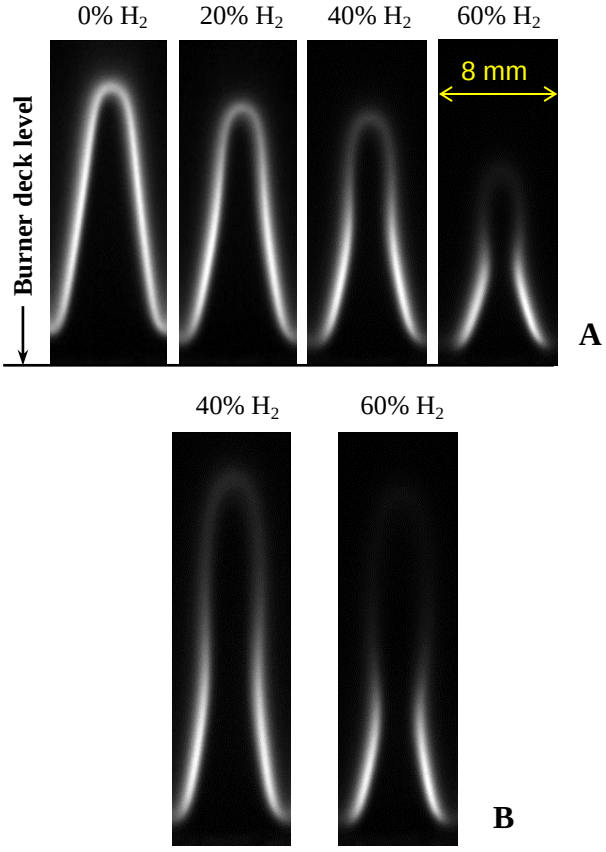

Figure 2 **A, B**. Images of the central flame for mixtures with different vol. hydrogen content in the fuel. Mixture with burning velocities S_b = 10 cm·s^{-1} (**A**) and S_b = 7 cm·s^{-1} (**B**). Mixture velocity at the burner outlet: U_{mix} = 60 cm·s^{-1}.

Figure 2 shows selected flame images taken though the CH* filter, for mixtures with burning velocities of 10 cm·s^{-1} (Fig. 2A) and 7 cm·s^{-1} (Fig. 2B). It is seen in Fig. 2 that the flame base approaches closer to the burner deck when the hydrogen content in the fuel is increased, suggesting a corresponding increase of heat losses to the burner deck. As also seen in Fig. 2, for fixed values of $S_{b,}$ shorter flames with a, correspondingly, smaller flame surface area, were produced at higher hydrogen contents in the fuel. The net burning velocity defined as the ratio of the mixture volumetric flow to the flame surface area, therefore increased with increasing hydrogen content, despite the

fact that the theoretical burning velocity is constant. This observation shows that the effect of the flame stretch-induced preferential diffusion on the local burning velocity is non-linear along the flame. Indeed, from symmetry considerations, the tangential gas velocity component to the flame front is zero at the flame base locations (these locations correspond to the left and right boundaries of the flame front in Fig. 2). Taking into account that the flame is stationary, the last means that the net (integrated) flame stretch rate over the entire flame front in Fig. 2 is zero [8]. If the local burning velocity varied linearly with the local flame stretch, the net burning velocity and, therefore, the area of the flame front, would not change and would be equal to S_b. The fact that the flame area decreases with increasing hydrogen content in the fuel blend, means that overall burning velocity along the flame increases. Note that this happens despite the fact that flames with more hydrogen stabilize closer to the burner deck, suggesting the (negative) effect of the heat loss on net burning velocity increases.

It can be also observed in Fig. 2 that the flame front becomes more non-uniform with increasing hydrogen content in the fuel gas and decreasing equivalence ratio. The flame tip becomes weaker and longer, inflection points appear below the flame tip. The flame tip takes a bulbous shape, with larger bulb size for higher hydrogen content in the fuel, larger mixture velocity, and smaller equivalence ratio. The observed evolution of the flame tip shape is consistent with theoretical results of Buckmaster and Crowley [9]. Using instant reaction assumptions and single Lewis number assumptions. Taking into account gas thermal expansion, these authors predicted appearance of the inflection points near the flame tip for $Le < 1$ flames, as well as the bulbous shape of the flame tip at small values of the Lewis number. Although the flames studied in the present work may not be described by a single Lewis number, an increasing hydrogen content in the fuel gas is expected to lead to qualitatively similar effects as it would be in the case of decreasing Lewis number in a mixture with a single fuel gas. At the same time, to our knowledge, bulbous shapes of the Bunsen flame tip have not been reported in literature for single fuel mixtures with $Le < 1$, for example, for lean hydrogen-air flames or rich propane-air flames, see e.g. [4, 5]. For those flames, a continuous flame front without inflection points was observed at the flame tip for near-stoichiometric flames. Upon departure from stoichiometry, local flame extinction and flame tip opening was observed [4, 5].

For hydrogen-containing mixtures, the size of the bulbous flame tip (identified as the region where the CH* chemiluminescence is relatively weak) increased with increasing mixture inlet velocity. Larger mixture velocities correspond to a smaller angle between the flame shoulders. In implication to turbulent flames, the 2-D flame tip corresponds to a flame cusp (or a flame

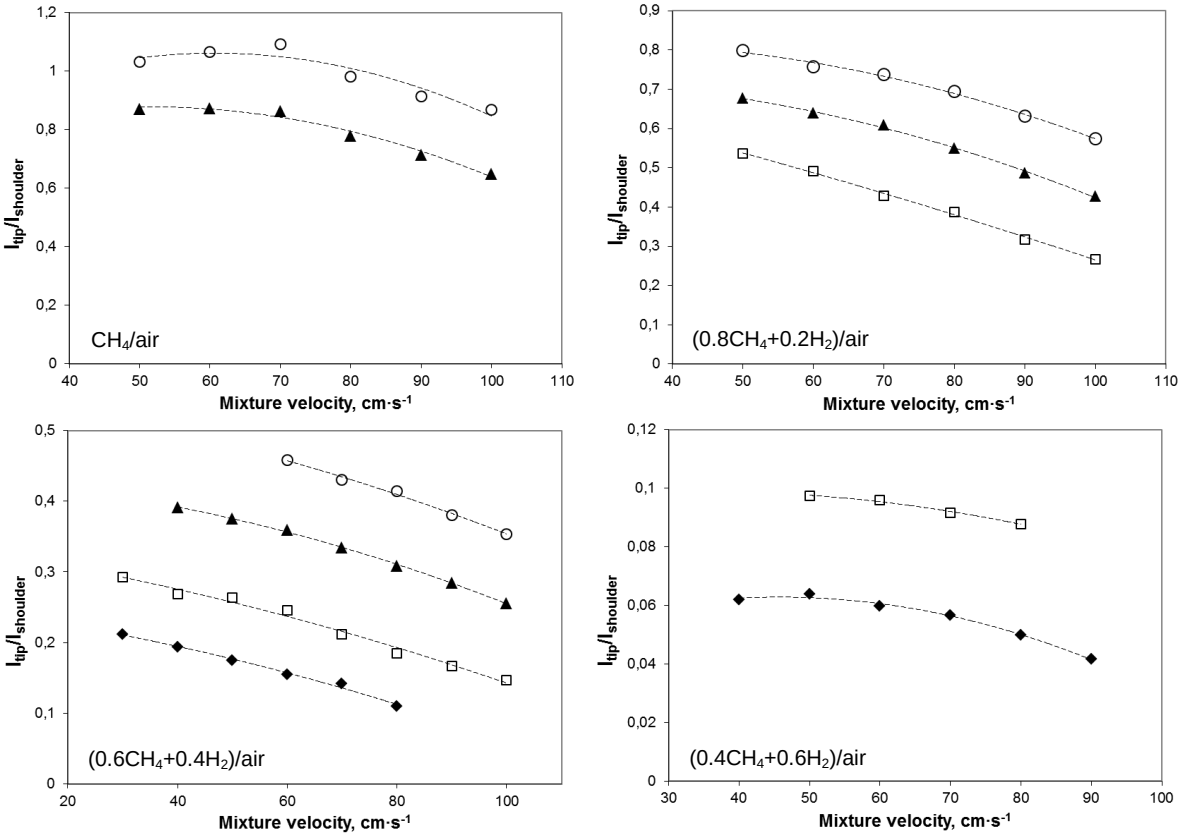

Figure 3. Ratio of local maximum intensities of the flame front image at the flame tip and flame shoulder. Flame images are taken through a CH* filter. Measurements performed for mixtures with theoretical burning velocity of the planar flame of 7 (♦), 10 (□), 15 (▲), and 20 (○) cm·s^{-1}.

fold). Therefore, the last observation means that deeper flame folds are expected to form on the front of a turbulent flame of such mixtures where the angle between adjacent flame fronts is larger. This, however, should be considered as an overall tendency, rather than as a strict rule, because the tip of a 2-D Bunsen flames does not reproduce non-stationary effects taking place during flame fold formation in a turbulent flame.

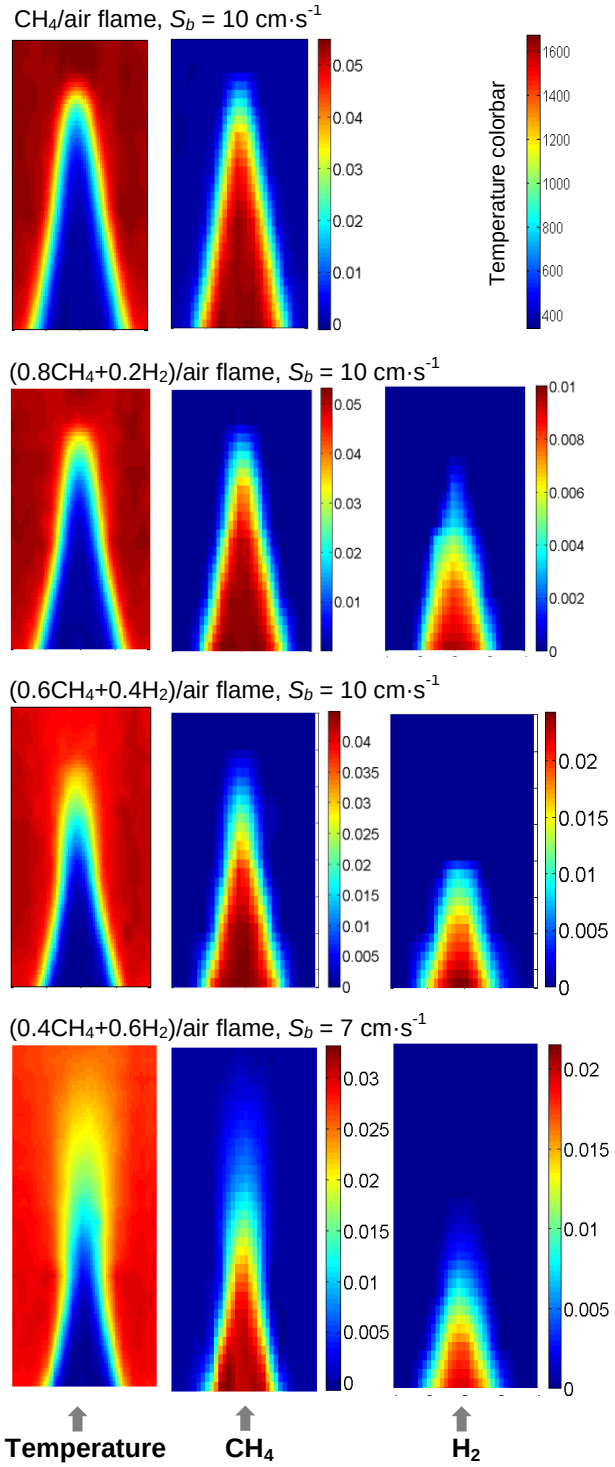

Figure 4. 2-D distributions of temperature, methane and hydrogen molar fractions, obtained by linear interpolation of line-wise Raman scattering measurements.

In all the studied flames, the flame front, identified as the local maximum of the flame luminosity, was clearly distinguishable at the flame tip for all tested flames. Flame tip opening has never been observed for studied flames, suggesting completeness of reaction.

Figure 3 shows the ratio of the flame front image intensities at the flame apex and at the location on the flame shoulder where the flame luminosity reaches the maximum, as a function of mixture velocity for different mixture compositions. This ratio can serve as a qualitative indicator of the strength of flame stretch-induced preferential diffusion effects on the local methane consumption rate at the flame tip. For each tested fuel composition and outlet mixture velocity, the measured intensity ratio is smaller for smaller values of the equivalence ratio. Probably, this observed tendency can be related to larger values of the characteristic

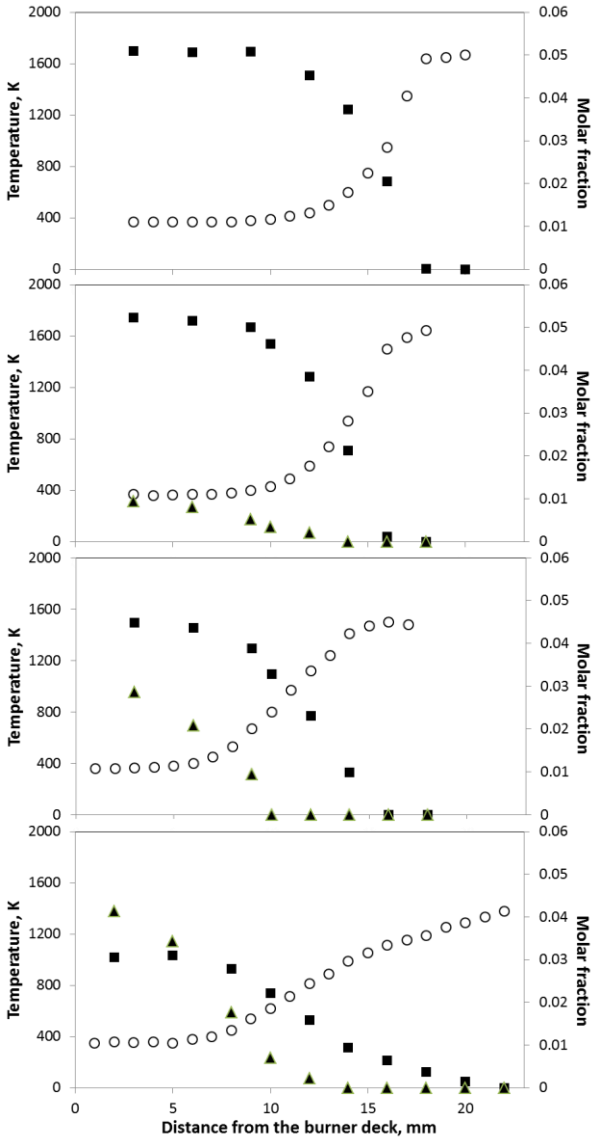

Figure 5. Vertical centerline profiles of temperature (○) and methane (■) and hydrogen (▲) molar fractions, measured by Raman scattering. Mixture compositions and order of flames from top to bottom are the same as in Fig. 4.

Karlovitz number at the flame tip for learner mixtures, which have a larger flame diffusion thickness. To prove this, however, measurements of gas velocities are required. It also can be seen in Fig. 3, that, for fixed values of the mixture velocity and of the theoretical burning velocity of a corresponding planar flame, the measured intensity ratio rapidly decreases with increasing the hydrogen fraction in the fuel. This is consistent with the fact that preferential diffusion effects becomes stronger as more hydrogen is added to the fuel. One can see in Fig. 3 that, with some exemptions, the measured intensity ratio decreases as the mixture inlet velocity becomes larger and the angle of the flame shoulder decreases.

Raman scattering measurements have been performed for CH_4/air, $(0.8CH_4+0.2H_2)$/air, and $(0.6CH_4+0.4H_2)$/air mixtures with S_b = 10 cm·s^{-1} (φ = 0.588, 0.569, and 0.528, correspondingly). Flames of the (0.4CH4+0.6H2)/air mixture with S_b = 10 cm·s^{-1} (φ = 0.45) exhibited some cellular instability at the flame base. Therefore, the $(0.4CH_4+0.6H_2)$/air mixture with lower burning velocity for the 1D flame, S_b = 7 cm·s^{-1} (φ = 0.45), has been chosen for Raman scattering measurements. Note that it was not possible to produce stable flames of mixtures corresponding to the value of S_b = 7 cm·s^{-1} either, as the corresponding methane-air flame was blown off.

Distributions of temperature and molar fractions of methane and hydrogen are shown in Fig. 4, measured by Raman scattering. Vertical centerplane profiles are shown in Fig. 5. A single color scale, shown in the right top corner in Fig. 3, is used for all temperature plots. In flames of mixtures containing 40% and 60% H_2 in the fuel, noticeable reduction of the flame temperature at the flame tip is seen, which is in accordance with numerical predictions of flame cusps in turbulent flames of hydrogen-methane-air mixtures [10, 11]. Flame temperature reduction at the flame tip is not observed for CH_4/air and $(0.8CH_4+0.2H_2)$/air mixtures, possibly, because it is below the accuracy of Raman measurements (about 50 K)

As seen in Fig. 4 and 5, methane molar fraction distributions in the flame interior region are similar, though with opposite sign, to the temperature distributions, which is a consequence of near-unity value of the Lewis number for methane. At the same time, in flames with the hydrogen addition, hydrogen dissipates from the flame core at much faster rate than methane does as the mixture approaches the flame fold and then flows inside it. No hydrogen is detected inside the upper part of the flame fold in flames of mixtures with 40% and 60% of H_2 in the fuel, suggesting that at the flame apex only methane burns. The behavior of molar fractions of hydrogen and methane in the flame fold are in qualitative agreement with results of [10, 11]. Distributions of methane consumption rates in a turbulent flame, computed by authors of [10], show a discernable continuous flame front in the flame fold regions even in the mixture containing 87.5% of hydrogen in the fuel blend. At the same time, gaps were observed at flame fold locations on simulated hydrogen consumption rate distributions for the same mixture, as well for a mixture with lower (75%) hydrogen content in the fuel.

Distributions of methane and hydrogen in a $(0.6CH_4+0.4H_2)$/air turbulent flame predicted by direct numerical simulation are compared in [11]. These authors found that hydrogen dissipates from the flame fold region at a much faster rate compared to methane. At the same time, opposite from results of the present work for a similar fuel blend (Figs. 4 and, 5) the presence of noticeable amount of hydrogen is predicted inside the whole interior of the flame fold in [11]. It should be noted, however, that the (0.6CH4+0.4H2)/air flame used for Raman measurements in the present paper was much leaner than the flame simulated in [11] (φ = 0.528 in the present work against φ = 0.7 in [11]).

It is seen in Fig. 2, 3 and 4 that in flames with a high hydrogen content, the preheating of the mixture flowing along the flame centerlines begins well before the mixture reaches the reaction front. Apparently, this preheating is due to the diffusion heat flux from two sides of the fronts of the flame fold formed at the tip of the flame. The observed preheating may result in a large value of the local burning velocity at the flame apex, despite the depletion of the mixture due to negative flame stretching. This, at least in part, might explain the non-linear response of the net burning velocity on the stretch rate variations along the flame. To verify this hypothesis, however, gas velocity measurements are necessary.

Conclusions

Distributions of temperature and major chemical species in flame cusps, represented by tips of 2D Bunsen flames of hydrogen-methane-air mixtures have been measures using spontaneous Raman scattering. To characterize flame shapes, sizes and, qualitatively, local consumption rates of methane, flame images were taken though an interference CH* filter. Lean flames of mixtures of air with methane and with hydrogen-methane fuel blends containing 20, 40, and 60% of hydrogen have been studied.

All studied flames had a continuous luminous front on images registered through the CH* filer, suggesting the absence of local extinction at the flame tip (cusp). The degree of local weakening of the flame by negative stretch at the flame tip has been qualitatively characterized by the ratio of flame front image intensities measured at the flame tip and flame shoulder. The effect of the negative flame stretch was found to increase with hydrogen content in the fuel blend. For a fixed fraction of hydrogen in the fuel, relative weakening of the flame tip becomes more significant at lower equivalence ratios and larger mixture velocities at the burner exit.

Inflection points form at flame tip when hydrogen is present in a mixture. In flames of mixtures with 40 and 60% of hydrogen in the fuel, the flame tip/fold takes the

shape of an elongated (up to 10-12 mm) bulb. Mixture preheating begins right after the mixture enters the fold. Inside the fold, hydrogen gets totally depleted well before the mixture reaches the flame apex, suggesting that only methane reacts at the apex of those highly-rich hydrogen flames. The obtained results are in qualitative agreement with numerical predictions of the structure of flame folds in turbulent flames of hydrogen-methane-air mixtures [9].

Acknowledgements

This work was partially supported by the Dutch Technology Foundation STW (Projects 11616 and 13549)), which is part of the Netherlands Organization for Scientific Research (NWO), and which is partly funded by the Ministry of Economic Affairs.

Literature

1. J.B. Bell, R.K. Cheng, M.S. Day, I.G. Shepherd, Proc. Comb. Inst., 31 (2007) 1309–1317.
2. M.S. Day, J.B. Bell, X. Gao, P. Glarborg. Proc. Comb. Inst., 33 (2011) 1591–1599.
3. B. Lewis, G. von Elbe, Combustion, Flames, and Explosions of Gases, Academic Press, NY, 1961.
4. M. Mizomoto, Y. Asaka, S. Ikai C. K. Law, Proc. Comb. Inst., 27 (1984) 1933-1939.
5. A.V. Sepman, V.V. Toro, A.V. Mokhov, H.B. Levinsky, Appl. Physics B, 112 (2013) 35-47.
6. J.A. van Oijen, L.P.H. de Goey, Combust. Sci. Tech. 161 (2000) 113-137.
7. G.P. Smith, D.M. Golden, M. Frenklach, N.W. Moriarty, B. Eiteneer, M. Goldenberg, C.T. Bowman, R.K. Hanson, S. Song, W.C. Gardiner, Jr., V.V. Lissianski, Z. Qin http://www.me.berkeley.edu/gri_mech/
8. Y. Shoshyn, L.P.H. de Goey, in Proc. of the 4th European Combustion Meeting, Vienna, Austria, 14-17 april 2009
9. J. Buckmaster, A. B. Crowley, J. Fluid Mech., 131 (1983) 341-361.
10. M.S. Day, X. Gao, J.B. Bell, Proc. Comb. Inst. 33 (2011) 1601–1608.
11. A.W. Vreman, J.A. van Oijen, L.P.H. de Goey, R.J.M. Bastiaans, Int. J. Hydr. Energ. 34 (2009) 2778 – 2788.